Pure Appl. Chem., Vol. 74, No. 3, pp. 337–347, 2002.

Nonequilibrium discharges in air and nitrogen plasmas at atmospheric pressure*

Charles H. Kruger‡, Christophe O. Laux, Lan Yu, Denis M. Packan, and Laurent Pierrot

High Temperature Gas Dynamics Laboratory, Mechanical Engineering Department, Stanford University, Stanford, CA 94305, USA

Abstract: Diffuse glow discharges were produced in low temperature (<2000 K) atmospheric pressure air and nitrogen plasmas with electron number densities in excess of 10^{12} cm^{-3}, more than six orders of magnitude higher than in thermally heated air at 2000 K. The measured discharge characteristics compare well with the predictions of a two-temperature kinetic model. Experimental and modeling results show that the steady-state electron number density exhibits an S-shaped dependence on the electron temperature, a behavior resulting from competition between ionization and charge-transfer reactions. Non-Maxwellian effects are shown to be unimportant for the prediction of steady-state electron number densities. The power requirements of DC discharges at atmospheric pressure can be reduced by several orders of magnitude using short repetitive high-voltage pulses. Between consecutive pulses, the plasma is sustained by the finite rate of electron recombination. Repetitive discharges with a 100-kHz, 12-kV, 10-ns pulse generator were demonstrated to produce over 10^{12} electrons/cm^3 with an average power of 12 W/cm^3, 250 times smaller than a DC discharge at 10^{12} cm^{-3}.

INTRODUCTION

There are interesting applications of nonequilibrium diffuse discharges in molecular gases, particularly air, at atmospheric pressure. Desirable conditions are electron densities greater than 10^{12} cm^{-3} at gas temperatures less than 2000 K. To increase the electron number density without significantly heating the gas, energy must be added in targeted fashion. One method is to apply the energy addition to the free electrons by means of an electrical discharge. Such discharges have been successfully applied in atmospheric pressure air [1] to produce stable, diffuse plasmas with electron densities of up to 10^{11} cm^{-3}, but higher electron densities are considered difficult to obtain owing to instabilities and arcing effects [1].

In this article, we first describe our two-temperature chemical kinetic models of air plasma discharges. The influence of departures from a Maxwellian distribution of the free-electrons is examined with a simplified collisional-radiative model coupled with a Boltzmann solver for a nitrogen plasma. We then present results of experiments in atmospheric pressure air and nitrogen, using either cold or preheated process gas, in which the electron density was raised to above 10^{12} cm^{-3} by means of a DC discharge. Finally, we present results from pulsed discharge experiments in which electron densities of more than 10^{12} cm^{-3} in air are produced with approximately 12 W/cm^3, a factor 250 times lower than the power required for a DC discharge.

*Lecture presented at the 15th International Symposium on Plasma Chemistry, Orléans, France, 9–13 July 2001. Other presentations are presented in this issue, pp. 317–492.

‡Corresponding author

TWO-TEMPERATURE KINETIC MODELS

Two-temperature chemical kinetic models were developed to understand the mechanisms governing ionization and electron recombination in discharges produced by an applied electric field. The two temperatures are the electron temperature, T_e, and the gas temperature, T_g. Rate coefficients describing the air plasma chemistry were derived using the Weighted Rate Coefficient (WRC) method [2]. In this method, rate coefficients are calculated as a weighted average of elementary rates over the internal states of atoms and molecules. Elementary rate coefficients are calculated from cross-section data assuming Maxwellian velocity distribution functions for electrons and heavy-particles, and are then averaged over the internal energy levels, assuming Boltzmann distributions at the electronic temperature T_{el}, vibrational temperature T_v, and rotational temperature T_r. It is further assumed that $T_{el} = T_e$ and $T_r = T_g$. The remaining parameter, T_v, can only be determined by means of a collisional-radiative (CR) model of vibrationally specific state-to-state kinetics. We have developed a CR model to determine the relation between T_v and T_g and T_e in atmospheric pressure nitrogen plasmas [3]. It was shown [4] that the steady-state concentrations determined with a two-temperature kinetic model assuming that $T_v = T_g$ are in close agreement with the CR model predictions in the range of electron densities of interest here, and are at worse within a factor 5 of the CR model predictions at electron densities greater than about 10^{17} cm^{-3} (region B in Fig. 1). In contrast, the often-used assumption $T_v = T_e$ would produce steady-state electron number densities several orders of magnitude greater than those obtained with the CR model at the electron densities of interest. We extend these results to atmospheric pressure air by calculating all WRC rate coefficients with the assumption $T_v = T_g$. Two-temperature kinetic calculations were made with the CHEMKIN solver [5] modified to account for two-temperature rates [6]. Electron attachment reactions are neglected because the equilibrium concentrations of O_2^- and O^- are negligible relative to the concentration of electrons in atmospheric pressure air above ~1500 K.

Two-temperature chemistry simulations

We consider first the case of an air plasma in equilibrium at 2000 K and 1 atm at time zero when an elevated electron temperature is instantaneously prescribed, in an idealized way modeling an electrical discharge in a reactor section. Species concentrations are calculated for various electron temperatures while keeping the gas temperature constant at 2000 K. For $T_e \geq 6000$ K, electron-catalyzed ionization reactions become important and the steady-state electron number density increases rapidly with the electron temperature. The small circles in Fig. 1 represent the predicted steady-state electron number densities as a function of the electron temperature in atmospheric pressure air at fixed $T_g = 2000$ K. An

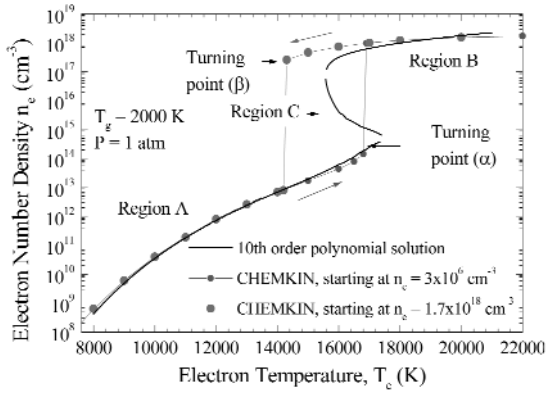

Fig. 1 Steady-state electron number densities predicted by CHEMKIN and analytical solution.

abrupt change in electron density occurs for $T_e \cong 17\,000$ K where the predicted steady-state electron number density suddenly increases from ~10^{14} to ~4×10^{17} cm^{-3}.

In the reverse case where steady-state electron concentrations are calculated from an initial composition given by the steady-state solution at $T_g = 2000$ K and $T_e = 22\,000$ K (corresponding to $n_e^{(t=0)} \cong 10^{18}$ cm^{-3}), the predicted steady-state electron number densities (large circles in Fig. 1) start by decreasing along the same upper curve as in the previous case, but instead of the abrupt decrease at 17 000 K, continue their smooth decrease until the electron temperature reaches ~14 000 K. When T_e is further decreased below 14 000 K, the steady-state electron density abruptly decreases and then retraces the solution of the previous case. Thus the electron number density as a function of the electron temperature presents a hysteresis. Detailed examinations of the mechanism and rates were made to determine the main reactions controlling the steady-state electron number density in regions A and B [6].

Region A

When the electric field is applied, the electron concentration rises rapidly as a result of three-body electron-impact ionization of N_2 and O_2 and of electron-impact dissociation of O_2 followed by electron-impact ionization of O. The charged species produced by these processes undergo rapid charge transfer to NO^+, mainly via $O^+ + N_2 \Rightarrow NO^+ + N$. The main electron removal reaction is the two-body dissociative recombination reaction $NO^+ + e \Rightarrow N + O$. When the concentration of NO^+ becomes sufficiently large, the rate of dissociative recombination balances the rate of electron production and the plasma reaches steady state. Thus in Region A, the termination step of the ionization process is the two-body recombination of a molecular ion.

Region B

The initial electron number density increase occurs by the same processes as in region A, i.e., electron-impact ionization of N_2, O_2, and O. Unlike in Region A, however, charge-transfer reactions are not fast enough to produce sufficient NO^+ for the rate of dissociative recombination to balance the ionization rate. This is because the latter reactions are controlled by the gas temperature, whereas electron impact ionization reactions are controlled by T_e. The limit between Regions A and B corresponds approximately to the electron temperature for which the rate of the charge transfer reaction $O^+ + N_2 \Rightarrow NO^+ + N$ is comparable with the rate of avalanche ionization by electron impact. Above this critical electron temperature, the avalanche ionization process continues until all molecular species are dissociated. Eventually the rates of three-body electron recombination reactions balance the rate of ionization, and steady state is reached.

Analytical solution

The kinetics in Regions A and B can be described with a simplified subset of reactions that take into account the dominant channels discussed in the foregoing paragraph. With this simplified mechanism, the steady-state concentrations of major species are obtained by solving the species conservation equations of electrons, O_2, O, NO^+, O^+, O_2^+, and N_2^+. By elimination of n_O, n_{O_2}, n_{O^+}, $n_{O_2^+}$, $n_{N_2^+}$, and n_{NO^+}, a tenth-degree polynomial in n_e is obtained, with coefficients that only depend on T_g, T_e, $n_{O_2}^{(0)}$, and $n_{N_2}^{(0)}$. The roots of this polynomial are plotted in Fig. 1 along with the CHEMKIN predictions obtained with the full kinetic mechanism. As shown in Fig. 1, the analytical solution generally agrees with the CHEMKIN predictions in regions A and B, but it also exhibits an extra solution (Region C) that could not be attained with CHEMKIN. If CHEMKIN is initialized with a point in Region C, a new steady-state electron number density is obtained on either the lower (Region A) or upper (Region B) limb of the steady-state CHEMKIN curves.

For comparison with the kinetic model, the "S-shaped" curves of n_e vs. T_e have been converted into more readily measured current density vs. electric field by use of Ohm's law and the electron energy equation. The latter incorporates the results of the collisional-radiative model to account for non-elastic energy losses from the free electrons to the molecular species. The electrical discharge charac-

teristics of Fig. 4 in the following section exhibit variations that reflect both the S-shaped dependence of electron number density vs. T_e, and the dependence of the inelastic energy loss factor on the electron temperature and number density.

DC DISCHARGES

To test the predicted S-shaped curve, DC discharge experiments were conducted with low-temperature, atmospheric-pressure flowing air and nitrogen plasmas. The experimental setup is shown in Fig. 2. Process gas is injected in the discharge region with low initial temperature and electron density. Spectroscopic and electrical measurements are made of the temperature, electrical conductivity, and electron density as a function of the applied discharge current.

DC discharge experiments in air

Figure 3a shows a photograph of the air plasma plume at a temperature of approximately 2000 K in the region between the two electrodes without the discharge applied. Figure 3b shows the same region with a DC discharge of 5.2 kV and 200 mA applied. The interelectrode distance is 3.5 cm. The bright center region in Fig. 3b corresponds to the discharge-excited plasma. The discharge diameter is approxi-

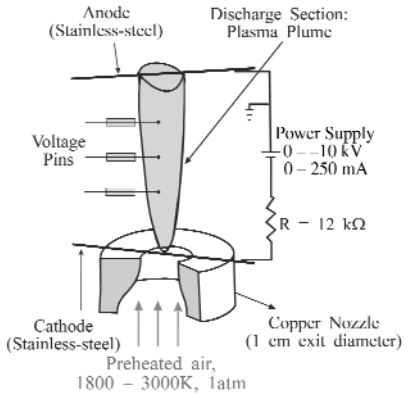

Fig. 2 DC discharge schematic.

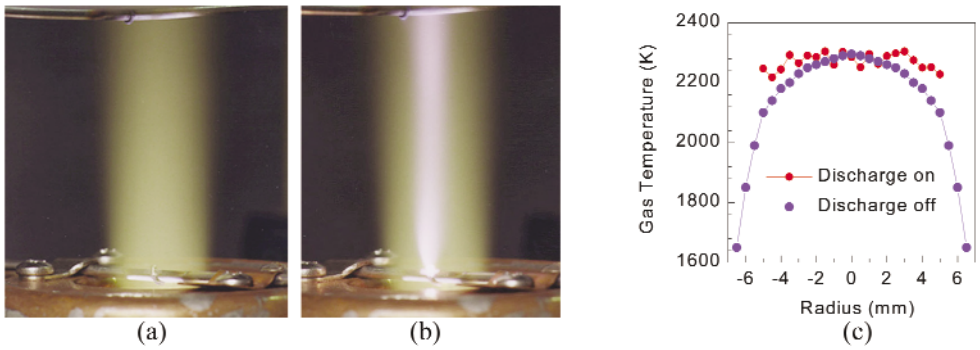

Fig. 3(a). Air plasma at 2000 K without discharge. 3(b). Air plasma at 2000 K with discharge (1.4 kV/cm, 200 mA). Interelectrode gap: 3.5 cm. Measured electron number density in the discharge region: ~10^{12} cm^{-3}. 3(c). Rotational temperature profiles at 1.5 cm above the bottom electrode.

mately 3.2 mm (full width at half-maximum intensity of the N_2 C–B emission profile) and the electron concentration determined from electrical conductivity measurements is approximately 10^{12} cm^{-3}. The temperature profile was measured from rotational lines of the OH (A–X) transition in the case without the discharge, and of the N_2 (C–B) transition with the discharge applied. The centerline temperature decreases from 2300 K at the cathode to 2020 K at the anode when no discharge is applied. With the discharge, the measured temperature remains approximately constant at 2300 K along the discharge axis. Radial temperature profiles measured at 1.5 cm downstream of the cathode are shown in Fig. 3c. It appears that the discharge does not noticeably increase the rotational temperature of the plasma under these conditions.

The measured discharge characteristics for plasma temperatures ranging from 1800 to 2900 K are shown in Fig. 4. Also shown are the predicted discharge characteristics at temperatures of 2000 and 3000 K. A more detailed description of our theoretical work on discharge characteristics may be found in ref. 6. Good agreement is obtained between the measured and predicted discharge characteristics over a range of experiments spanning over three orders of magnitude in current density.

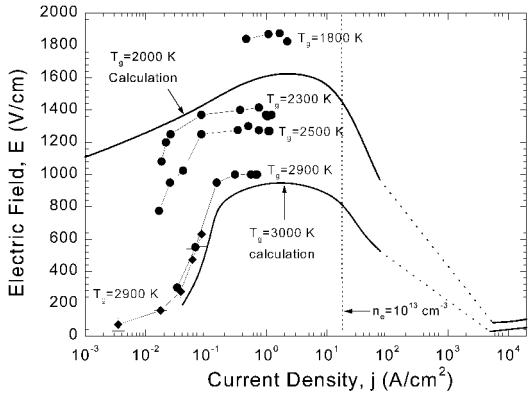

Fig. 4 Measured (symbols) and predicted DC discharge characteristics in air at 1 atm.

Discharge experiments in nitrogen

Discharge experiments were also conducted with atmospheric pressure nitrogen either at room temperature or preheated to temperatures between 1800–2250 K. For the room temperature experiments, nitrogen is injected between the electrodes at a velocity of about 2 m/s. The gas heats up to temperatures between 2200 and 2800 K as a result of discharge-induced Joule heating. For the experiments with preheated nitrogen, the gas is injected at about 450 m/s. Owing to the relatively fast flow rate, the gas temperature remains practically constant in the discharge region. The discharge diameter is about 1.7 mm in the room-temperature nitrogen experiments, and 5 mm in preheated nitrogen. The difference in discharge diameters is due to the larger radial thermal gradients in cold nitrogen than in the preheated flow. In all cases, the measured cathode fall is about 300 V, which is typical of a glow discharge. The measured discharge characteristics are shown in Fig. 5, along with the characteristics calculated with the nitrogen CR model. As shown in Fig. 5, the measured characteristics support the results of the chemistry and discharge models.

The foregoing calculations were performed using Maxwellian distribution functions for the translational energies of the electrons and heavy particles. To investigate the limitations of this simplification, the electron Boltzmann equation was solved for nitrogen plasmas in conjunction with a somewhat simplified form of the collisional-radiative model. The results, shown in Fig. 6, do not differ significantly from those with the Maxwellian version.

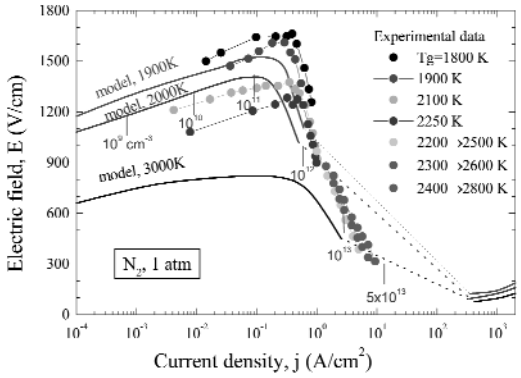

Fig. 5 Measured (symbols) and predicted DC discharge characteristics in nitrogen at 1 atm.

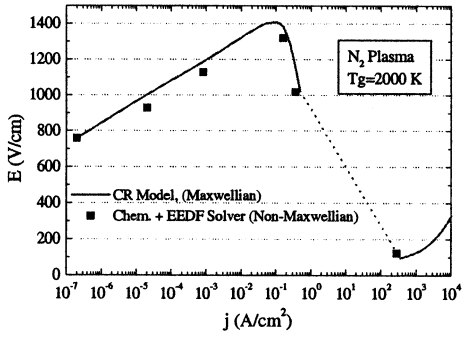

Fig. 6 Predicted discharge characteristics in atmospheric pressure nitrogen at 2000 K.

PULSED DISCHARGES

As the power required to sustain elevated electron densities with DC discharges is large, a power reduction strategy based on pulsed electron heating was explored. This strategy is illustrated in Fig. 7. Short voltage pulses are applied to increase the electron number density. After each pulse, n_e decreases according to electron recombination processes. When n_e reaches the minimum desired value, a second pulse is applied. The average electron density obtained with this method depends on the pulse duration,

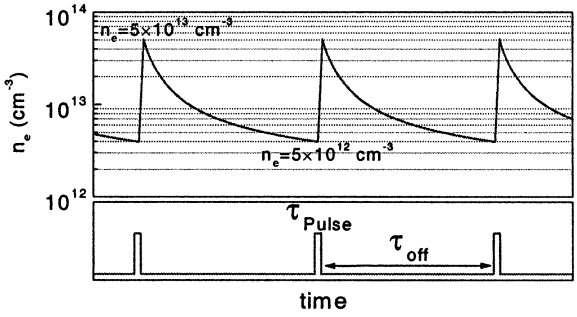

Fig. 7 Repetitively pulsed strategy.

pulse voltage, and the interval between pulses. This approach is analogous to the pulsed discharges of refs. 7 and 8, which operated at lower pressures and lower electron densities in CO_2-laser mixtures.

As seen in the previous section, DC discharges can maintain $n_e \geq 10^{12}$ cm^{-3} in atmospheric pressure air with electric fields producing an electron temperature on the order of 1 eV. To produce the same average electron density with short (1–10 ns)-pulsed discharges, a higher electron temperature of about 3–5 eV is required. Although the corresponding field is higher than for a DC discharge, the ionization efficiency is much larger in the pulsed case than in the DC case because the energy lost to nitrogen molecules, per electron created, is several orders of magnitude smaller at T_e = 3–5 eV than at 1 eV. This coupled with the finite electron recombination time allows the power budget to be dramatically reduced with pulsed discharges. It may be shown [9] that the power reduction afforded by the repetitively pulsed approach relative to DC is given by:

$$R \cong \frac{k_{ion}(T_{e,Pulse})N}{k_{DR}n_e^*} \times \alpha^2 e^{\alpha}\left(e^{\alpha}-1\right)^{-2} \times \left(\frac{T_{e,DC}}{T_{e,Pulse}}\right)^{3/2}$$

where $\alpha \equiv k_{ion}N\tau_1$, and where k_{ion} is the species-weighed rate coefficient for electron impact ionization of O_2, N_2, and O, k_{DR} the rate coefficient for dissociative recombination of NO^+, N the total number density of species, τ_1 the pulse length, n_e^* the average electron number density produced by the repetitively pulsed discharge, and $T_{e,DC}$ and $T_{e,Pulse}$ represent the electron temperatures produced by the DC and pulsed discharges, respectively.

Experiments with a single pulse

To test the pulsing scheme, experiments were conducted [9] in atmospheric pressure, 2000 K air using a pulse-forming line capable of generating a 10 ns rectangular pulse with peak voltage up to 16 kV. To experimentally simulate the conditions of a repetitively pulsed discharge, the initial elevated electron number density generated by the "previous" pulse is created by means of a DC discharge in parallel with the pulser. The circuit schematic is shown in Fig. 8. With a DC voltage of 2 kV and current of 150 mA, the initial electron density is 6.5×10^{11} cm^{-3}. A 10-kV, 10-ns pulse is superimposed to further increase the electron density. The measured discharge diameter of about 3 mm is comparable with the diameter of the DC discharge (Fig. 9). The temporal variation of plasma conductivity was measured from the voltage across the electrodes and the current density through the plasma. The electron density increases from 6.5×10^{11} to 9×10^{12} cm^{-3} during the pulse, then decays to 10^{12} cm^{-3} in about 12 μs (Fig. 10). The average measured electron density over the 12-μs duration is 2.8×10^{12} cm^{-3}.

Figure 10 shows a comparison of the measured electron number density with the predictions of our two-temperature model. The predictions agree well with the measured electron decay time of 12 μs. This decay time is consistent with the dissociative recombination time of NO^+ predicted to be 8.7 μs without the DC background. Thus, these results provide validation of our chemical kinetic model of the recombination phase.

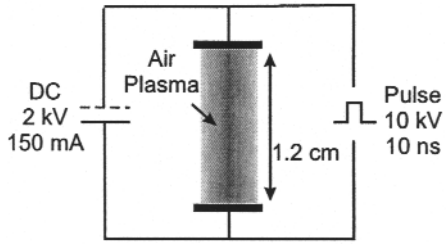

Fig. 8 Schematic of the combined pulsed and DC discharge experiments.

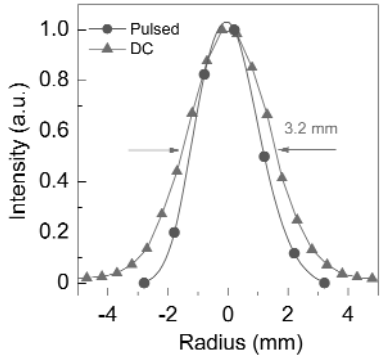

Fig. 9 Spatial extent of the plasma produced with pulsed and DC discharges, determined from N_2 C–B emission.

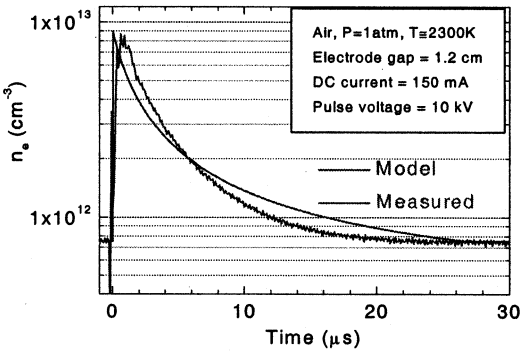

Fig. 10 Temporal electron density profile in the 10 ns pulsed discharge.

Experiments with 100-kHz repetitive discharge

The success of the proof-of-concept experiments conducted with the single pulse discharge led us to investigate the generation of air plasmas with a repetitively pulsed discharge. A repetitive pulser capable of generating 10-ns pulses, with peak voltages of 3–12 kV and pulse repetition frequencies up to 100 kHz was acquired from Moose-Hill/FID Technologies. This pulser operates with a solid-state opening switch or Drift-Step Recovery Diode (DSRD). The experimental set-up is shown in Figs. 11 and 12. The discharge is applied to preheated, LTE air at atmospheric pressure and 2000 K. The DC circuit in parallel with the pulser was used only to determine the electron number density from the plasma conductivity. In regular operation, the DC circuit is disconnected and the discharge operated with the pulser only.

A photograph of the repetitively pulsed discharge in operation in atmospheric pressure preheated (2000 K) air is shown in Fig. 13. The diffuse character of the discharge was confirmed with time resolved (1.5 ns frames every 2 ns) measurements of plasma emission during the pulse. The diameter of the discharge is approximately 3.3 mm. Figure 14 shows the measured temporal variations of the electron density during three cycles of the pulsed discharge. The electron number density varies from 7×10^{11} to 1.7×10^{12} cm^{-3}, with an average value of about 10^{12} cm^{-3}. The power deposited into the plasma by the repetitive discharge was determined from the pulse current (measured with a Rogowski coil), the voltage between the electrodes (6-kV peak) minus the cathode fall voltage (measured to be 1525 V by varying the gap distance), and the measured discharge diameter. The peak pulse current was

240 mA. The power deposited is found to be 12 W/cm^3, consistent with the theoretical value of 9 W/cm^3 for an optimized pulsed discharge producing 10^{12} electrons/cm^3. It is lower, by a factor of 250, than the power of 3000 W/cm^3 required to sustain 10^{12} electrons/cm^3 with a DC discharge.

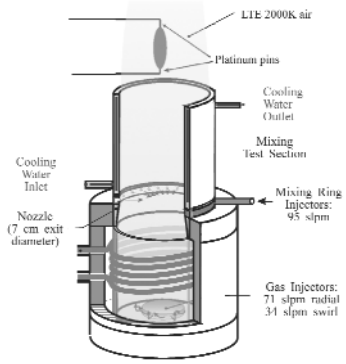

Fig. 11 Set-up for repetitive pulse discharge in air at 2000 K, 1 atm.

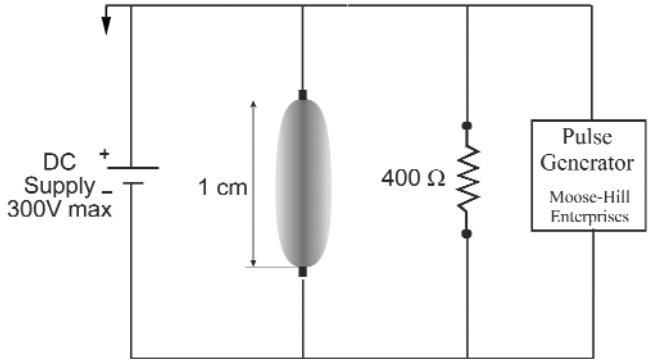

Fig. 12 Repetitive pulse discharge circuit schematic (DC circuit applied only for conductivity measurements).

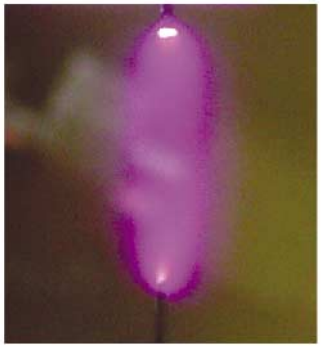

Fig. 13 Photograph of repetitive pulse discharge in air at 2000 K, 1 atm. Interelectrode gap: ~1 cm.

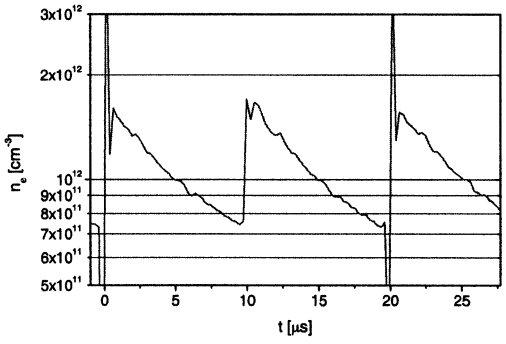

Fig. 14 Electron number density measurements in the repetitive pulse discharge.

CONCLUSIONS

Two-temperature ($T_e > T_g$) kinetic models accounting for ionizational, chemical, vibrational and electronic nonequilibrium, and incorporating a collisional-radiative model with over 11 000 transitions have been developed to understand the mechanisms of ionizational nonequilibrium in atmospheric pressure air and nitrogen electrical discharges. These models predict that (even) at atmospheric pressure energetic electrons driven by the discharge can establish and maintain electron-density nonequilibrium of over six orders of magnitude. An unexpected result is an "S-shaped" dependence of n_e on T_e at steady state for a given gas temperature. This behavior results from a transition between predominately molecular ions to atomic ions at a critical value of T_e and values of n_e above about 10^{14} cm^{-3}. Above this critical value of T_e, the electron density increases dramatically so that three-body recombination can maintain a steady state. Departures from a Maxwellian distribution of the free-electrons were found to have a negligible effect on the predicted steady-state characteristics, at least for the case of a nitrogen plasma.

The feasibility of such nonequilibrium discharges was demonstrated in atmospheric-pressure nitrogen and air at both room temperature and around 2000 K with electrode spacings of cm scale. Stable, diffuse DC discharges have been achieved at atmospheric pressure for a range of gas flow and temperature conditions including those which produce n_e of 10^{12} to 10^{13} cm^{-3} without significant gas heating. Good agreement between theoretical and measured discharge characteristics has been obtained for both air and nitrogen discharges over a wide range of conditions including electron densities greater than 10^{12} in air and 10^{13} in nitrogen.

To reduce the power required to maintain such nonequilibrium, the finite electron recombination time (~10 μs) has been exploited by means of pulsed discharges of 10-ns duration. Both single-shot and repetitively pulsed diffuse discharges at 100 kHz have been demonstrated, with power reductions of over two orders of magnitude for average electron densities greater than 10^{12} cm^{-3}. Current experiments are exploring larger-scale discharges with multiple electrodes.

ACKNOWLEDGMENTS

This work was funded by the Director of Defense Research & Engineering (DDR&E) within the Air Plasma Ramparts MURI Program managed by the Air Force Office of Scientific Research, under the cognizance of Dr. Robert J. Barker.

REFERENCES

1. E. E. Kunhardt. *IEEE Trans. Plasma Science* **28**, 189–200 (2000).
2. L. Pierrot, C. O. Laux, C. H. Kruger. *Prog. Plas. Proc. Mat.* Begell House, NY, 153–159 (1999).
3. L. Pierrot, L. Yu, R. J. Gessman, C. O. Laux, C. H. Kruger. *AIAA 99-3478*, 30th PDL Conf., Norfolk, VA (1999).
4. L. Yu, L. Pierrot, C. O. Laux, C. H. Kruger. *Plasma Chem. Plasma Proc.* **21**, 483–503 (2001).
5. R. J. Kee, F. M. Rupley, J. A. Miller. *CHEMKIN-II.* Sandia Report SAND89-8009 (1989).
6. C. O. Laux, L. Yu, D. M. Packan, R. J. Gessman, L. Pierrot, C. H. Kruger, R. N. Zare. *AIAA 99-3476*, 30th PDL Conf., Norfolk, VA (1999).
7. J. P. Reilly. *J. Appl. Phys.* **43**, 3411–3416 (1972).
8. A. E. Hill. *Appl. Phys. Lett.* **22**, 670–673 (1973).
9. M. Nagulapally, G. V. Candler, C. O. Laux, L. Yu, D. M. Packan, C. H. Kruger, R. Stark, K. H. Schoenbach. *AIAA 00-2417*, 31st PDL Conf., Denver, CO, 2000.